Effect of Clay on Immiscible Morphology of Poly(butylene terephthalate)/Polyethylene Blend Nanocomposites

Defeng Wu,[1,2] Chixing Zhou,[2] Ming Zhang[1]

[1]*School of Chemistry & Chemical Engineering, Yangzhou University, Jiangsu 225002, China*
[2]*School of Chemistry & Chemical Engineering, Shanghai Jiaotong University, Shanghai 200240, China*

Received 4 November 2005; accepted 19 December 2005
DOI 10.1002/app.24088
Published online in Wiley InterScience (www.interscience.wiley.com).

ABSTRACT: Polymer blend nanocomposites containing poly(butylene terephthalate) (PBT), polyethylene (PE), and organoclay were prepared by direct melt compounding. Their immiscible morphologies were investigated using electron microscopy, X-ray diffraction, and parallel plate rheometry. The PE domain sizes were reduced when the polar PBT phase was continuous (PBT/PE = 60/40) because the clay tactoids effectively prevented the coalescence of the dispersed PE domains. However, when the PBT component presented domains dispersed in the rich PE matrix (PBT/PE = 40/60), the addition of clay (>2 wt %) changed the phase morphology into a novel cocontinuous one, which was further confirmed by rheological measurements. The existence of clay tactoids led to a sharp enhancement in the viscosity of the PBT phase, changing the viscosity ratio between the PBT and PE phases remarkably, which may have promoted the phase inversion. As a result, clay had significant effects on the morphology of the polymer blend.
 J Appl Polym Sci 102: 3628–3633, 2006

Key words: nanocomposites; blend; morphology; rheology

INTRODUCTION

Polymer-layer silicate nanocomposites (PLSNs) have attracted great interest from industry and academia because they have frequently exhibited unexpected properties over the past decade, which are well reflected by the numerous publications devoted to PLSNs.[1–6] Recently, many research works have begun to focus on polymer blends with clay nanocomposites.[7–13] From those results it can be concluded that the dispersed clay platelets presented the behavior of selective localization in the polar polymer phase and played a compatibilizer-like role, reducing the dispersed nonpolar polymer phase size. However, those works mainly studied blends in which the rich polar polymer component presented a continuous phase morphology.

Rheometry has recently been proved to be a powerful tool for investigating the internal microstructures of nanocomposites.[14–16] The rheological behavior of intercalated poly(butylene terephthalate) (PBT)/clay nanocomposites was studied In our previous work, and the results showed that the formation of the percolated tactoids network distinctively influenced the terminal viscoelastic response.[17] Moreover, the enhancement in the density and intensity of the percolation network structure because of the addition of the epoxy resin as a compatibilizer led to a large change in the linear rheological properties of PBT/clay nanocomposites.[18–20] To study the kinetics of PBT melt intercalation under an oscillatory shear field, we prepared a multilayered sample with alternatively superposed PBT and polyethylene (PE)/clay sheets to investigate the whole hybridization process.[21] An immiscible morphology was found in the PBT/PE/clay nanocomposites in that work. The results from transmission electron microscopy and rheological measurements showed that clay tactoids were mainly dispersed in the polar PBT phase, presenting a selective localization. In the present work we are interested in investigating the effect of clay on the immiscible phase structure of polymer blends with different component ratios. To achieve this goal, we prepared PBT/PE/clay nanocomposites by melt mixing and then conducted morphology and rheology studies on those samples. This communication reports the formation of a novel cocontinuous morphology in PBT/PE blends that is due to the addition of clay, relating the linear rheological behaviors to the internal phase structure in the polymer blend/clay nanocomposites.

Correspondence to: D. Wu (dfwu@yzu.edu.cn).
Contract grant sponsor: National Natural Science Foundation of China; contract grant numbers: 20174024, 50373034.
Contract grant sponsor: Foundation of Jiangsu Provinicial Key Program of Physical Chemistry, Yangzhou University.

EXPERIMENTAL

Materials preparation

The PBT used in this study was a commercial product (1097, number-average molecular weight = 19,200) of

XinChen Synthetic Material Co. Ltd. Organoclay (DK2-1) was supplied by Fenghong Clay Co. Ltd. and modified with methyl tallow bis(2-hydroxyethyl) ammonium. The PE was a commercial linear low-density blow-molding grade (Q400, Shanghai Petrochemical Co. Ltd.), which has a nominal density of 0.9222 $\pm$ 0.0015 g/cm^{-3} and a melt index of 4.0 $\pm$ 0.8 (ASTM D 1238). PBT/PE/clay nanocomposites were prepared by the direct melt compounding of PBT and PE with organoclay in a Rheomix-600 mixer (Haake Rheocord 900) at 230°C and 50 rpm for 10 min, followed by compression molding. A PE/clay sample was prepared under the same conditions for comparison. The compositions of the composites are listed in Table I. All materials were dried at 80°C under a vacuum for 24 h before being used.

Morphology characterization

The degree of swelling and the interlayer distance of the clay in the samples were determined by X-ray diffraction (XRD). The experiments were performed using a Rigaku Dmax-rC diffractometer with a copper target and a rotating anode generator, operating at 40 kV and 100 mA. The scanning rate was 2°/min from 2° to 10°. The morphologies of the fractured surfaces of the samples were investigated using scanning electron microscopy (SEM) on a Hitachi S-2400 microscope with a 15-kV accelerating voltage. The PBT/PE/clay sample mixed for different times was rapidly taken out of the Rheomixer and kept in liquid nitrogen for some time to produce a frozen morphology. Then, it was brittle fractured in the normal direction of mixing for morphology measurements. An SPI sputter coater was used to coat the fractured surfaces with gold for enhanced conductivity.

Figure 1 shows the XRD results for all the composites. The d_{001} peak of the organoclay powder is observed at 3.70°. Compared with that of the clay powder, the d_{001} peak location of clay in the PE/MMT composite has nearly no movement, whereas there were shifts to lower angles of 2.42° and 2.56° in the annealed BEM and EBM samples, respectively. This elucidates that in the PE/MMT composite there was no PE chain crawl into the interlayer of clay. However, for the annealed BEM and EBM, the d_{001} distance expands to 3.53–3.72 nm, which confirms that the PBT chain has intercalated into clay tactoids during melt mixing, forming the intercalated structure.

TABLE I
Compositions and Abbreviations of Prepared Hybrids

	Composition (wt %)		
Sample	PBT	PE	Organoclay
BEM	60	40	8
BE	60	40	0
EBM	40	60	8
EBM2	40	60	2
EB	40	60	0
PBT/clay	100	0	6

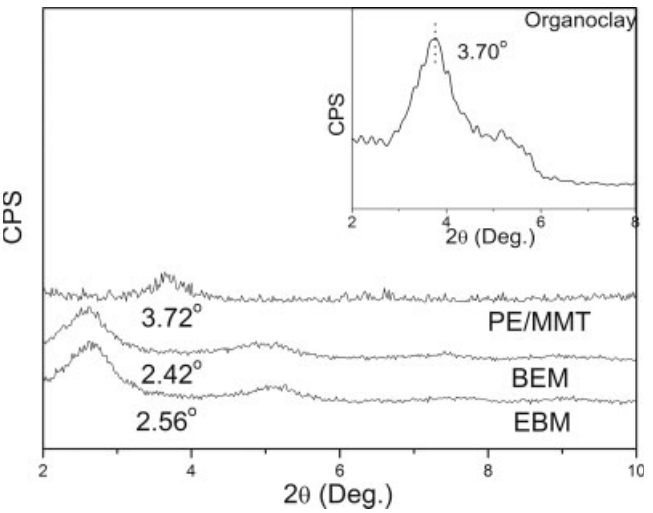

Figure 1 XRD patterns for organoclay clay and composites.

Rheological measurements

Rheological measurements were carried out in a small amplitude oscillatory frequency sweep (SAOS) mode on a rheometer (Gemini 200 rheometer, Bohlin Co.) equipped with a parallel plate geometry using 25-mm diameter plates. All measurements were performed with a 200 FRTN1 transducer at a lower resolution limit of 0.02 g cm. The sample was annealed at 230°C in the rheometer in a nitrogen environment. The frequency sweep was carried out during the annealing period. All sweeps were conducted at a strain of 1%.

RESULTS AND DISCUSSION

The SEM images of the fracture surfaces of the BEM and BE samples are provided in Figure 2. The spherical PE domains (about 5–10 μm) are dispersed in the PBT matrix, and the interfacial adhesion between the PE and the PBT matrix is weak [Fig. 2(a)]. However, the addition of 8 wt % clay to the blends causes a reduction in the size of the PE particles, as can be seen in Figure 2(b). This suggests that the clay tactoids suppress the coalescence and the agglomeration of the PE particles and, in contrast, the increased melt viscosity with the formation of intercalated nanocomposites also prevents the domains from aggregating. Compared to that of BE, the weight ratio between PE and PBT in the EB sample changes to 60/40. As a result, the PBT phase presents spherical domains dispersed in the PE matrix that are due to its lower viscosity and higher polarity, as shown in Figure 2(c).

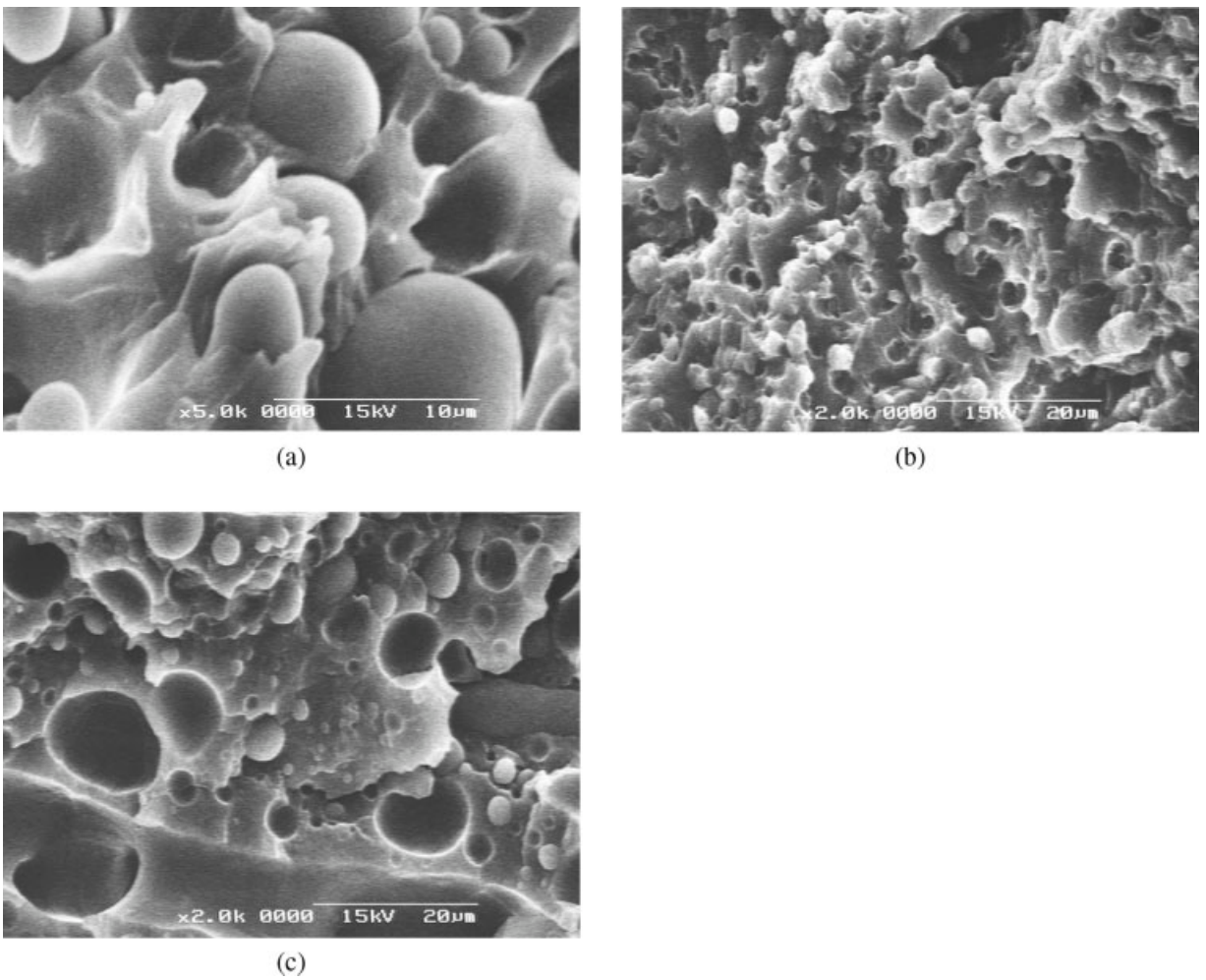

Figure 2 SEM images of (a) the BE sample at an original magnification of 5000, (b) the BEM sample at an original magnification of 2000, and (c) the EB sample at an original magnification of 2000.

Because the intercalated clay tactoids have selective localization in the PBT phase,[20] the final microstructure of the BEM sample may be schematically described as that in Figure 3(a): the detached tactoids are mainly dispersed in the continuous PBT phase together with the small spherical PE domains (about 2–5 μm). In the EBM sample the small PBT particles comprising tactoids dispersed in the PE matrix may be its final morphology, as shown in Figure 3(b).

We found that the linear viscoelastic response of PLSNs to SAOS can sensitively reflect the change of internal microstructures. Figure 3(d) gives the dynamic elastic modulus (G') for all samples. In contrast to that of BE, the EB sample presents a higher G' because of its higher loadings of the PE component. Both of them slightly deviate from terminal behavior ($1gG' \sim 1g\omega$) at the lower frequencies, which can attribute to their internal immiscible microstructure. With the addition of 8 wt % clay, the low-frequency G' of the BEM sample increases about 3 orders compared with that of the BE sample and the dependencies of G' on ω decrease sharply in the terminal zone, exhibiting a distinct plateau at the low frequencies. This solidlike viscoelastic response of PLSNs results from the formation of a supermicrostructure, percolated tactoids network.[14,15,17]

Provided that the internal morphology of the EBM sample is as depicted in Figure 3(b), the tactoids can only interact with those in the same PBT particle. As a result, the percolation network will not form on the whole scale [in contrast to Fig. 3(a)] because the small PBT domains are separated from each other by a continuous PE matrix. However, Figure 3(d) shows that the low-frequency G' of EBM increases sharply compared with that of the EB sample and presents a remarkable solidlike response, indicating the formation of a percolated tactoids network. This suggests that the internal morphology of the EBM sample might not be as depicted in Figure 3(b).

SEM images of EBM samples at different magnifications are presented in Figure 4(a,b). Surprisingly, a distinct cocontinuous phase structure can be observed in EBM. The PBT phase is not the dispersed domain like that in the EB sample, but it transforms into a continuous one that is tangled randomly with the continuous

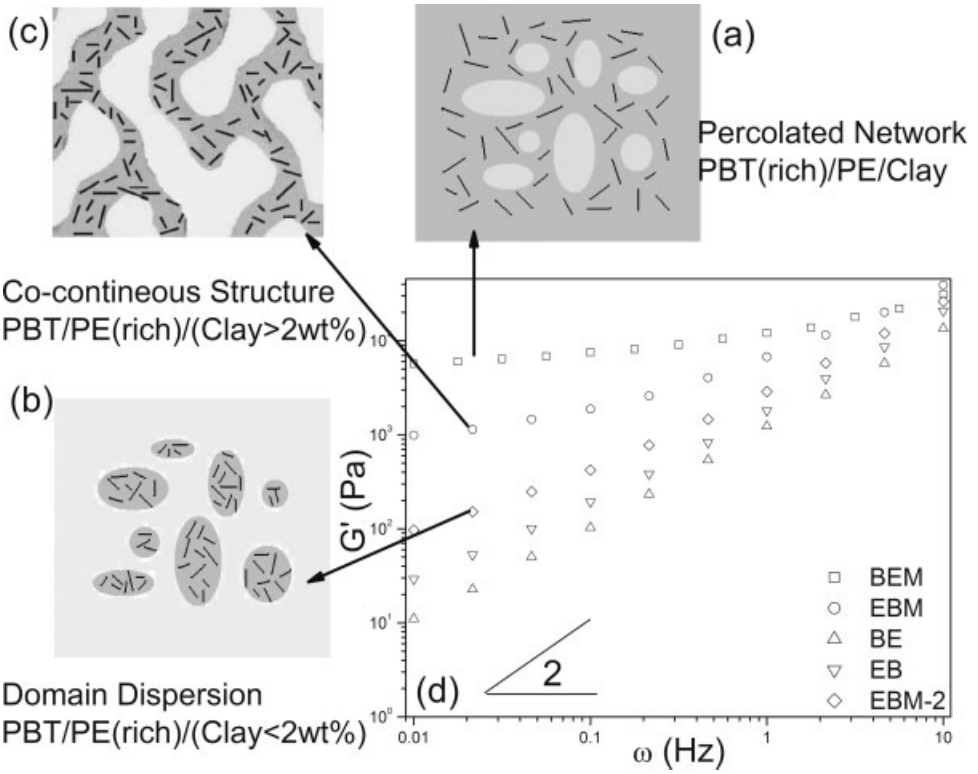

Figure 3 A schematic diagram for (a) BEM, (b) domain dispersed EBM2, and (c) a cocontinuous EBM sample. The dark gray areas are the PBT phase, the light gray areas are the PE phase, and the black lines are the tactoids. (d) The dynamic storage moduli (G') for all samples.

PE phase. Based on the selective localization of clay tactoids, the internal morphology of EBM is schematically shown in Figure 3(c). The tactoids are dispersed in the continuous PBT phase. Therefore, they can effectively ''feel'' one another through the continuous PBT matrix because of their friction or collision, forming a percolation network structure, which leads to a solidlike response of the EBM sample in SAOS experiments. However, from the schematic diagram of the morphologies for BEM [Fig. 3(a)] and EBM [Fig. 3 (c)], it is suggested that the percolated tactoids network in EBM is not as perfect and compact as that in the BEM sample, despite their identical clay loadings and similar expansion of the gallery height. As a result, although the higher viscosity component, PE, is the rich component of EBM, it presents a lower G' and higher terminal slope at low frequencies than that of BEM.

To further investigate the mechanism of the morphological change in polymer blends with the addition of clay, SEM measurements were conducted on

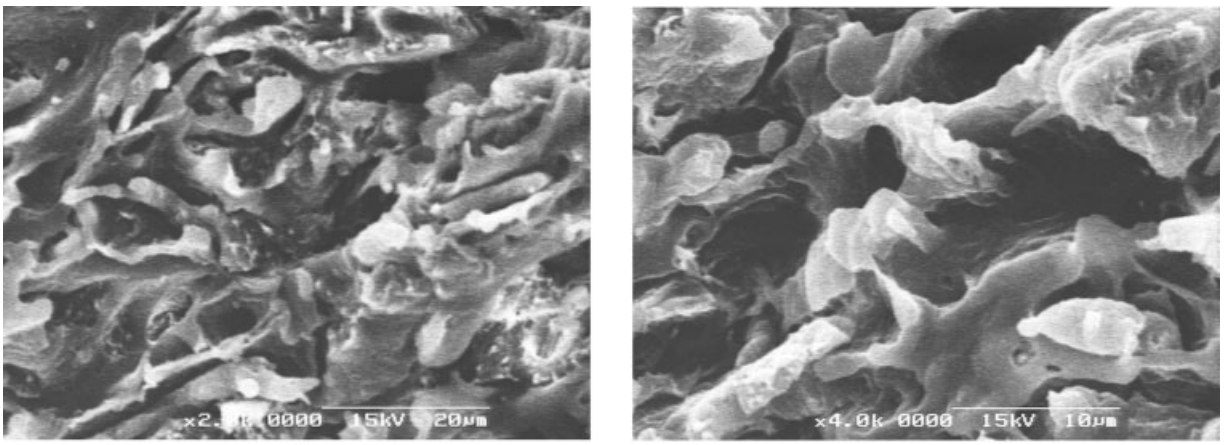

(a) (b)

Figure 4 SEM images of the EBM samples at original magnifications of (a) 2000 and (b) 4000.

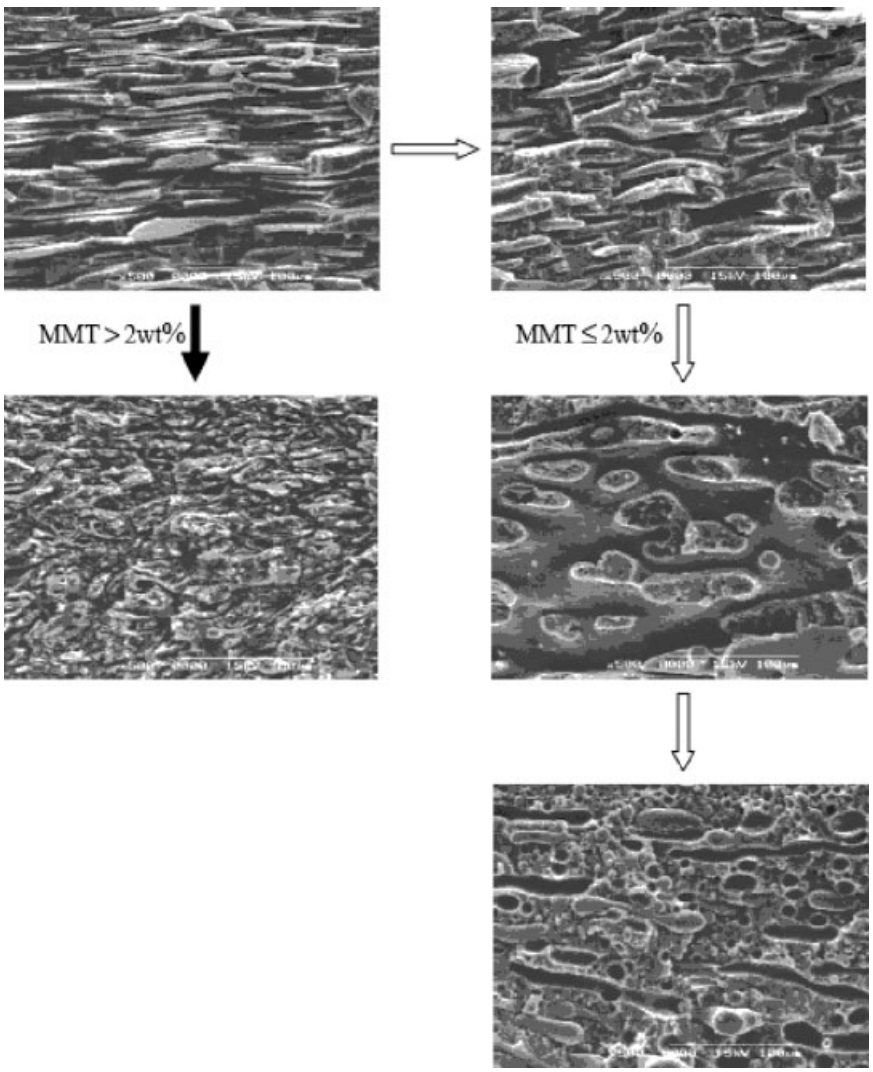

Figure 5 The effect of clay loadings on the morphology evolution of the PBT/PE (40/60) composite in the melt process.

the PBT/PE/clay samples mixed for different times (PBT/PE = 40/60), as can be seen in Figure 5. At the beginning of mixing, the composite presents a typical alternatively superposed multilayer morphology because the immiscible PBT and PE phases are selectively removed. Then, the continuous PBT phase is broken off gradually in the strong shear field because of its lower weight ratio and viscosity. With lower clay contents ($\leq$ 2 wt %) or without clay the broken PBT phase will evolve into a dispersed sea-island morphology and finally transform into spherical domains, achieving equilibrium between breakdown and coalescence between the particles (hollow arrow, Fig. 5). However, those intergradations are difficult to find in the morphology evolution of those composites with higher clay loadings ($>$ 2 wt %). The cocontinuous phase structure is the final morphology (solid arrow, Fig. 5.)

It is believed that the cocontinuous structure of a binary polymer blend can be formed within a composition region near the phase inversion point, and the relative melt viscosities of the two components is the dominant factor influencing the composition range.[22,23] In our previous work[17] the percolation threshold of PBT was about 3 wt %, meaning that as the clay loadings achieved a critical fraction or above, the interactions between tactoids was sharply enhanced, resulting in the formation of a percolation network. Therefore, for EBM, with melt blending, more highly anisotropic plateletlike clay tactoids rapidly detach from primary particles. Conversely, the physical jamming of those tactoids tied with PBT chains results in a remarkable enhancement in the viscosity of the PBT phase, raising the viscosity ratio between the PBT and PE phases, which also may retard the PBT phase from breaking down to some extent. The results from dynamic viscosity measurements are provided in Figure 6. For the PBT matrix the dynamic viscosity is about 200 PA s in the linear viscoelastic region whereas that of the PE matrix is

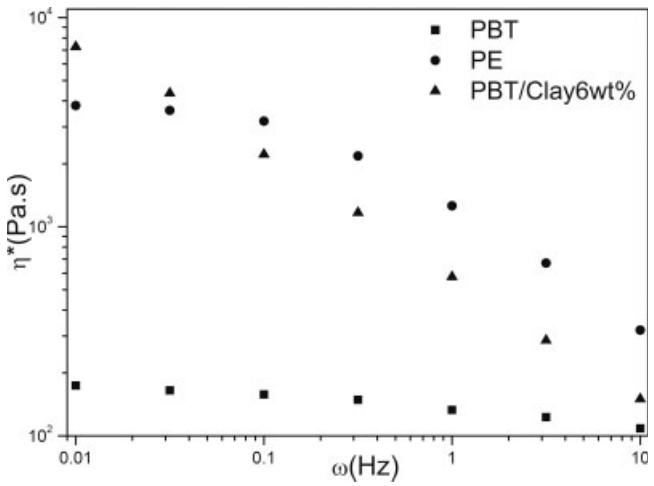

Figure 6 A comparison of the dynamic viscosities for PBT and PE matrices as well as the PBT/clay nanocomposite.

about 4000 PA s, which is almost 20 times that of PBT. Although the clay loadings for the PBT/clay (6 wt %) sample may be much less than that located in the PBT phase of the EBM sample, its dynamic viscosity in the lower frequencies is higher than that of neat PE. Therefore, the existence of clay tactoids in the EBM sample changes the viscosity ratio between the PBT and PE phases remarkably, resulting in phase inversion.

However, in lower clay loadings ($\leq$ 2 wt %), the amount of tactoids in the EBM2 sample is not enough to raise the viscosity ratio to the phase inversion point. The final morphology of the PBT/PE blend still presents domain or sea-island dispersion, as shown in Figure 5, which is further confirmed by the SAOS measurements. Observe from Figure 3(d) that the lower frequency G' of EBM2 is higher than that of the EB sample. However, both of them are in the same order, and the G' curves of EBM2 still present a distinct dependency on the frequencies in the terminal region. This suggests that the percolated tactoids network might not form on the whole scale in the EBM2 sample. Only those tactoids in the same PBT particle can interact with one another, as depicted schematically in Figure 3(b).

At this stage of the study, we only report a novel cocontinuous morphology in the PBT/PE/clay nanocomposites and discuss a possible mechanism for the formation of a cocontinuous phase structure by the rheological approach and SEM. The results may not be sufficient to ascertain all the factors influencing the immiscible morphologies of the PBT/PE blend nanocomposite. An experimental study relating the steady and transient rheological behavior of a PBT/PE/clay nanocomposite to its phase structure will be reported in the future, which hopefully will provide a specific insight into phase inversion.

CONCLUSIONS

Nanocomposites of PBT/PE/clay were prepared by direct melt compounding. The results from the morphology characterization showed that the PE domain size was reduced when the polar PBT phase was continuous (PBT/PE = 60/40). The existence of clay tactoids suppressed the coalescence and agglomeration of the PE particles. However, when PBT presented domain dispersion in a rich PE matrix (PBT/PE = 40/60), the addition of clay (> 2 wt %) changed the morphology into a novel cocontinuous one. The enhancement in the viscosity of the PBT phase that was due to the percolation of those tactoids tied with PBT chains led to a remarkable increase in the viscosity ratio between the PBT and PE phases, which may be a possible mechanism in the formation of the cocontinuous structure in the blend.

This work was supported by research grants from the National Natural Science Foundation of China and the Foundation of Jiangsu Provinicial Key Program of Physical Chemistry at Yangzhou University.

References

1. Vaia, R. A.; Janndt, D. K.; Kramer, E. J. Macromolecules 1995, 28, 8080.
2. Krishnamoorrti, R.; Vaia, R. A.; Giannelis, E. P. Chem Mater 1996, 8, 1728.
3. Usuki, A.; Kato, M.; Okada, A.; Kurauchi, T. J. J Appl Polym Sci 1997, 63, 137.
4. Wu, Z. G.; Zhou, C. X.; Qi, R. R.; Zhang, H. B. J Appl Polym Sci 2002, 83, 2403.
5. Li, X. C.; Kang, T.; Cho, W. J.; Lee, J. K.; Ha, C. S. Macromol Rapid Commun 2001, 21, 1306.
6. Wu, D. F.; Zhou, C. X.; Xie, F.; Mao, D. L.; Zhang, B. Polym Polym Compos 2005, 13, 61.
7. Li, Y. J.; Shimizu, H. Polymer 2004, 45, 7381.
8. Mehrabzadeh, M.; Kamal, M. R. Polym Eng Sci 2004, 44, 1152.
9. Chow, W. S.; Mohd, Z. A.; Karger, J. J Polym Sci Part B: Polym Phys 2005, 43, 1198.
10. Lee, K. Y.; Goettler, L. A. Polym Eng Sci 2004, 44, 1103.
11. Yoo, Y.; Park, C.; Lee, S. G.; Choi, K. Y.; Kim, D. S.; Lee, J. H. Macromol Chem Phys 2005, 206, 878.
12. Li, Y. J.; Shimizu, H. Macromol Rapid Commun 2005, 26, 710.
13. Khatua, B. B.; Lee, D. J.; Kim, H. Y.; Kim, J. K. Macromolecules 2004, 37, 2454.
14. Galgali, G.; Ramesh, C.; Lele, A. Macromolecules 2001, 34, 852.
15. Li, J.; Zhou, C. X.; Wang, G. J Appl Polym Sci 2003, 89, 3609.
16. Li, J.; Zhou, C. X.; Wang, G.; Zhao, D. J Appl Polym Sci 2003, 89, 318.
17. Wu, D. F.; Zhou, C. X.; Xie, F.; Mao, D. L.; Zhang, B. Eur Polym J 2005, 41, 2199.
18. Wu, D. F.; Zhou, C. X.; Xie, F.; Mao, D. L.; Zhang, B. Polym Degrad Stabil 2005, 87, 511.
19. Wu, D. F.; Zhou, C. X.; Yu, W.; Xie, F. J Polym Sci Part B: Polym Phys 2005, 43, 2807.
20. Wu, D. F.; Zhou, C. X.; Yu, W.; Xie, F. J Appl Polym Sci 2006, 99, 340.
21. Wu, D. F.; Zhou, C. X.; Zheng H. J Appl Polym Sci, to appear.
22. Paul, D. R.; Barlow, J. W. J Macromol Sci Rev Macromol Chem 1980, C18, 109.
23. Utracki, L. A. J Rheol 1991, 35, 1615.